Available online at www.sciencedirect.com
SCIENCE DIRECT
Journal of Physics and Chemistry of Solids 66 (2005) 1539–1543
JOURNAL OF PHYSICS AND CHEMISTRY OF SOLIDS
www.elsevier.com/locate/jpcs

Trapping single electrons on liquid helium

P. Glasson[a], G. Papageorgiou[a], K. Harrabi[a], D.G. Rees[a], V. Antonov[a], E. Collin[a,b], P. Fozooni[a], P.G. Frayne[a], Y. Mukharsky[b], M.J. Lea[a,*]

[a]*Department of Physics, Royal Holloway, University of London, Egham, Surrey TW20 0EX, UK*
[b]*CEA, Saclay, France*

Abstract

Surface-state electrons on liquid helium, localised in quantum dots, have been proposed as condensed matter qubits. We now demonstrate experimentally that small numbers of electrons, including a single isolated electron, can be held in a novel electrostatic trap above the surface of superfluid helium. A potential well is created using microfabricated electrodes in a 5 μm diameter pool of helium. Electrons are injected into the trap from an electron reservoir on a helium microchannel. They are individually detected using a superconducting single-electron transistor (SET) as an electrometer. A Coulomb staircase is observed as electrons leave the trap one-by-one until the trap is empty. A design for a prototype quantum information processor using an array of electron traps on liquid helium is presented.

Keywords: A. Quantum wells; A. Surfaces; D. Surface properties; D. Electronic structure

1. Introduction

The search is on for an experimental implementation of quantum information processing (QIP), leading to a quantum computer (QC). One of many proposed QIP systems uses electrons on helium (EoH) as suggested by Platzman and Dykman [1]; these electronic qubits are excellent candidates theoretically. The Platzman and Dykman QC consists of an array of localised electrons on a liquid helium surface, controlled by individually addressed submerged electrodes.

The balance between the attraction of the electron's image charge and the Pauli repulsion from the helium surface, creates a vertical potential well $V(z)$. For zero applied vertical electric field, the quantised energy levels are equivalent to Rydberg states in the hydrogen atom, $E_j = -R_e/j^2$ where $R_e = 0.66$ me $V \approx 160$ GHz for electrons on liquid ^{4}He, and $j \leq 1$ is the quantum number. The electrons 'float' a considerable distance above the liquid surface (11 and 46 nm for the ground and first excited states respectively). The frequency difference between these first two levels is $f_R = (E_2 - E_1)/h = 120$ GHz. Because of the asymmetric form of the wavefunctions $\psi(z)$, there is a linear Stark effect: the energy levels change with an applied vertical electric field F_z, as confirmed by studies of the microwave absorption [2]. The $|0>$ and $|1>$ states of the qubit are assigned to the ground and first excited electronic Rydberg states. An electron can be excited from $|0>$ to $|1>$ with a microwave pulse at the frequency f_R. Individual qubits are tuned by voltages on the underlying electrodes. Quantum gates could be operated by tuning neighbouring qubits through mutual resonance, generating entangled quantum states in XOR, square-root-of-swap or other quantum gates. Read-out would project the qubits onto the Rydberg basis states. The electron spins might also be used as qubit states [3]. This system is now under intense experimental and theoretical investigation.

2. Linear qubit array

The fundamental physics of electrons on helium is well understood [4]. The operational parameters for electronic qubits on ^{4}He have been given theoretically [1]. Each electronic qubit would be localised in a parabolic trap, with an in-plane resonant frequency about 20 GHz (compared to a Rydberg frequency of ≈ 200 GHz, depending on F_z).

* Corresponding author. Tel.: +44 1784 443485; fax: +44 1784 472794.
E-mail address: m.lea@rhul.ac.uk (M.J. Lea).

0022-3697/$ - see front matter © 2005 Elsevier Ltd. All rights reserved.
doi:10.1016/j.jpcs.2005.05.052

The Rabi frequency (for 1-qubit operations, determined by the applied microwave power) would be of the order of 100 MHz. Electrons will decay, from the excited state to the ground state, by two-ripplon emission (estimated rate $10^3\ s^{-1}$; one-ripplon decay is suppressed in the traps), by phonon emission ($10^4\ s^{-1}$) and by interaction with the control electrodes ($<10^3\ s^{-1}$). The dephasing rates at 10 mK are estimated as $10\ s^{-1}$ (1-ripplon interactions, $\propto T^3$), $10^2\ s^{-1}$ (2-ripplons, $\propto T^3$) and $10^4\ s^{-1}$ (electrodes, $\propto T$). At 10 mK some 10^5 gate operations could be performed within the decoherence time.

An array of single-electron traps would be used for QIP, with a typical electron separation of about 1 μm. The Coulomb dipole interaction couples neighbouring qubits and can generate universal two-qubit gates. A typical clock frequency (for 2-qubit operations, determined by the qubit–qubit coupling) would be of the order of 100 MHz. Each qubit can be Stark tuned by individual sub-surface electrodes. This tuning is a key feature for QIP applications, especially as the Coulomb interaction between neighbours cannot be turned off. The most natural architecture is a linear array. Santos and Dykman [5] and Dykman et al. [6] have shown that a specific tuning sequence of on-site Rydberg energies can lead to the strong localisation of single-and many-particle stationary states, in a linear array of interacting qubits. This makes a scalable QC, where the inter-qubit interaction is not turned off, viable, since excitations do not decay between gate operations. Benjamin and Bose [7,8] also concluded that QIP with always-on interactions, and even with global control, can be efficiently executed using suitable tuning schemes for 1-D and 2-D arrays. Fowler et al. [9] have now shown that a linear nearest neighbour architecture, which is natural for EoH, can be efficiently used to implement Shor's algorithm. The number of qubits and gates required are, to first order, identical to architectures in which arbitrary pairs of qubits can interact together. There are several schemes for achieving this experimentally with EoH; a provisional design for a prototype linear array is presented below.

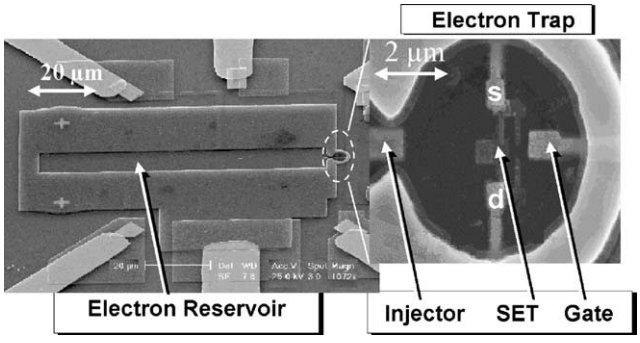

Fig. 1. A microelectronic device for trapping electrons on helium. (a) The electron reservoir and trap. (b) Expanded view of the electron trap, showing the Au gate electrode and an SSET with source (s) and drain (d) electrodes. The reservoir electrode projects into the trap to form an electron injector.

3. Electron trap on helium

We fabricated the novel microelectronic device, Fig. 1, on a Si/SiO_2 substrate, by depositing Al, Au and Nb electrodes to form shallow microchannels and pools defined by a guard electrode, proud of the surface. The bulk liquid helium level lies below the horizontal plane of the device. Capillary rise fills the channels with superfluid helium, which is held in place by surface tension. The helium depth is typically $d \approx 0.6$–0.8 μm, depending on the fabrication of individual devices. Free electrons are generated by thermionic emission from a pulsed filament. The electrons are stored on the helium surface in an electron reservoir, Fig. 1(a), which is a 10 μm wide helium microchannel [10] above a positively biased electrode at V_R.

The electrons are trapped on the helium surface in a 5 μm diameter circular helium pool, Fig. 1(b). The reservoir electrode slightly extends into the helium pool, acting as an injector to transfer electrons between the reservoir and the trap. A single-electron transistor (SET) lies beneath the helium surface in the electron trap, with source, drain, island and gate electrodes. Electrons in the trap are controlled by potentials on the electrodes, biased with respect to the surrounding guard electrode.

3.1. SET detection

The SET was fabricated using shadow evaporation. Al source and drain electrodes are connected to the SET island through $Al/Al_2O_3/Al$ tunnel barriers. It is operated below 0.5 K in the superconducting state at the Josephson-quasiparticle (JQP) peak in the I–V characteristic, with a source-drain voltage bias of 0.55 mV and a source-drain current $I_{SD} \approx 5$ nA.

Periodic Coulomb blockade oscillations (CBO) are observed in the dc current through the SET, as shown in Fig. 2, as the gate voltage V_g is swept. The dashed line shows the oscillations for an uncharged helium surface. Each oscillation corresponds to an extra electronic charge $-e$ induced in the SET island by capacitive coupling $Q_c^* = -C_{gi}V_g$ from the gate electrode (note that a positive gate voltage induces negative charge in the SET). The CBO

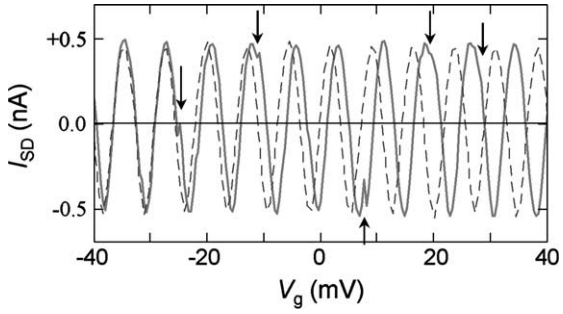

Fig. 2. CBO by sweeping V_g before (dotted) and after (solid) charging the helium surface. Jumps in the phase ϕ (see arrows) can be seen as free electrons enter the trap.

period, $\Delta V_g = 7.3$ mV, corresponds to $C_{gi} = e/\Delta V_g = 21.92$ aF. For an uncharged helium pool the relative long-term charge stability of the SET is about $0.01e$, comparable with good Si-based SETs [11]. The short-term $1/f$ noise is less important here than long-term drift. Random charge jumps and two-level fluctuators are sometimes observed.

The linear variation of Q_c^* with V_g provides a reference for the extra induced charge $\Delta Q^* = Q^* - Q_c^* = Q^* + C_{gi}V_g$ from surface-state electrons on the helium, where $Q^* = (\theta/2\pi)e$ is the total induced charge, determined from the phase ϕ of the CBO. The solid line in Fig. 2 shows the effects observed after the helium surface is charged. As V_g increases, the CBO deviates from the uncharged result, as extra charge is induced in the SET island. In general, these deviations can occur both as a slow shift of the CBO phase ϕ with respect to the uncharged phase and as discrete steps or phase jumps. Each surface-state electron in the trap induces a positive fractional charge in the SET island ΔQ_1^* and a phase shift $\Delta\phi_1$

$$\frac{\Delta Q_1^*}{e} = \frac{\Delta\phi_1}{2\pi} = \frac{c_1}{c_1 + c_2} > 0 \quad (1)$$

where c_1 and c_2 are the capacitive electrostatic couplings from the free charge to the island and the rest of the world respectively. The measured phase shift $\Delta\phi$ of the CBO makes the SET a very sensitive electrometer.

3.2. Filling the trap

Fig. 3 shows charging the trap by sweeping the reservoir voltage V_R. At point A (large positive V_R) there is no potential barrier between the reservoir and the electron trap (see Fig. 3b) and the trap is empty. As V_R is reduced, a potential barrier forms, but the trap remains empty (i.e. $\Delta Q^*/e = 0$). The potential energy of the surface-state electrons in the reservoir will be $E \approx -eV_R + ne^2d/\varepsilon\varepsilon_0 = -eV_e$ where n m^{-2} is the number density of the electrons on the reservoir. As V_R is reduced, this increases faster than the barrier potential. At point B the electrons spill over from the reservoir to fill the trap and the extra induced charge ($\Delta Q^*/e > 0$) on the SET island increases rapidly. This continues until $V_e = 0$ when electrons will no longer be confined by the grounded guard electrode. When V_R is swept positive again, electrons remain in the trap. At point C the potential energy of the electrons in the reservoir falls below the top of the barrier and the trapped electrons become isolated. As V_R increases further the barrier height decreases and electrons escape from the trap. For $V_R > 170$ mV, a series of small steps in $\Delta Q^*/e \approx 0.1$ can be identified (see insert) as electrons leave one at a time, until the trap is again empty at point A. The hysteresis observed here is a key demonstration of the filling and emptying of the electron trap.

3.3. Counting individual electrons

The CBO for a charged pool are shown in Fig. 2, while sweeping the gate voltage V_g. Jumps in the CBO phase ϕ are observed, relative to the oscillations for an uncharged pool. These correspond to positive steps in $\Delta Q^*/e$ above the uncharged baseline, as in the Coulomb staircase plotted in Fig. 4 where some five electrons are counted leaving the trap. Free electrons are attracted into the electron trap by a positive gate potential, inducing a positive charge on the SET island and giving a negative differential capacitance. By sweeping the electrodes negative we can remove all the surface-state electrons and recover the uncharged results.

The voltage, or Coulomb gap, required to increase the charge on a capacitor C by one electron is $\Delta V = e/(C + V(\mathrm{d}C/\mathrm{d}V)) = e/C^*$, allowing for variations in C with voltage V (i.e. from changes in the electron trap size).

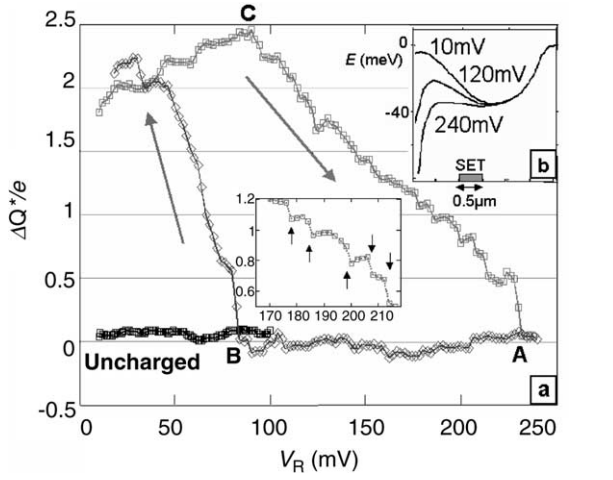

Fig. 3. (a) Filling the trap from the reservoir, showing the extra induced charge $\Delta Q^*/e$ on the SET island due to electrons in the trap as V_R is varied (see the text). The inset shows the charge steps. (b) The well potential for several values of V_R.

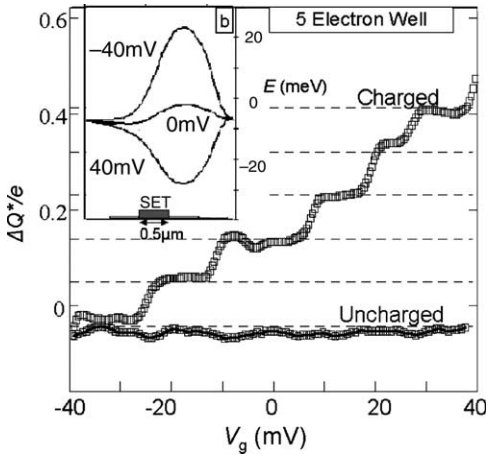

Fig. 4. Coulomb staircase for individual electrons. Charge steps (0.092 e) are seen in $\Delta Q^*/e$ as electrons leave the trap one by one until the trap is empty. The inset shows the potential profile of the trap for appropriate values of V_g.

If the gate electrode is coupled to the trapped electrons through a capacitance C_{ge} then a gate voltage increment is required to attract each extra electron into the trap. The data in Fig. 4 gives $C_{ge} \approx 13$ aF. The size of the charge steps is typically $0.092e = c_1/(c_1 + c_2)$ from Eq. (1) depending on the electrode potentials. An electrostatic model has been developed for this electron trap that reproduces these values and demonstrates the effects of the gate and reservoir potentials.

A simple estimate of the number of electrons N in a 2D trap is obtained from $N \approx CV_R/e$, where $C = 8\varepsilon_0 R$ is the capacitance of an unscreened charged pool of radius R, and $V(R)$ is the potential in the pool, where R and $V(R)$ are measured from the potential minimum. A 10 mV trap, of radius 1 μm, will hold $N \approx 4$ electrons.

3.4. The charging spectrum

The steps due to the addition and subtraction of individual electrons into the electron trap are clearly observed in each voltage sweep. However, the charging sequences in the dQ–V plots show hysteresis, depending on the direction of the voltage sweep, and a quite broad distribution of the voltage charging increments (the addition spectrum) in the hysteretic regime. Double electron steps are also observed, in which two electrons enter the trap simultaneously.

At low temperatures, Coulomb interactions between the electrons in the trap leads to localised electrons in specific structural arrangements, related to the 2D Wigner crystal or a Coulomb glass, depending on the strength of any disorder potential. In this region, the simple Coulomb gap capacitance model will only be an approximation. This has been studied in numerical simulations and a wide range of phenomena have been predicted. Bedanov and Peeters [12] calculated the charging energies for equilibrium trapped electrons in a 2D parabolic potential well, as shown in Fig. 5. But a metallic screening electrode close to a 2D electron sheet, as in our device, can lead to polaronic effects [13] in which the electronic spatial order is rearranged after the addition of extra electrons. One specific prediction was for simultaneous multiple electron addition, as seen in some semiconducting quantum dots [14]. Hysteresis and double electron addition follow from these ideas, as we observe experimentally. The distribution of the voltage charging increments (the addition spectrum) in the hysteretic regime, is in good agreement with the theoretical expression for a localised 2D Coulomb system with some disorder [15,16]. The experimental disorder implied by this could arise from the electron injection dynamics or from small variations in the trap potentials from substrate charges or surface-state electrons on the guard or reservoir.

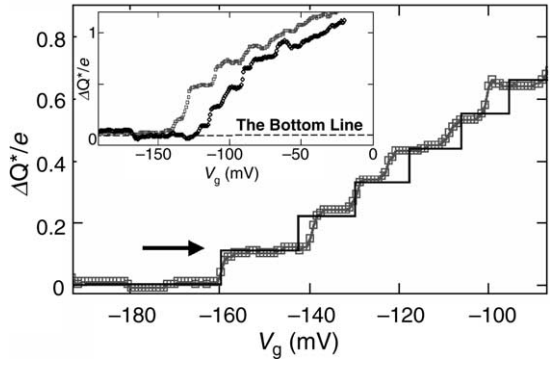

Fig. 5. Coulomb staircase for an electron trap. The solid line shows the charging sequence for a parabolic well [12]. The arrow shows the region where a single electron is trapped in the well. The inset confirms a base line (see text).

3.5. Single-electron trap

There is a clear region during each voltage sweep where a single electron is held in the trap, as shown in Fig. 5. The baseline (see inset) can be identified by reference to the uncharged CBO sweeps. This is the condensed matter equivalent of the trapped single particle systems first created by Hans Dehmelt [17] using electrons and positions who successfully trapped one specific positron, which he named Priscilla, for many months. It is also closely related to the trapped ion systems under development for QIP [18].

4. QIP with electrons on helium

These experiments now enable a novel design for a linear array quantum information processor, Fig. 6. An electron channel reservoir would feed electrons across an SET detector into a series of single-electron traps as qubits, controlled by electrodes and microwave pulses. The crucial read-out stage, following a processing sequence, first ionises those electrons in the upper $|1>$ state. The remaining $|0>$ electrons would then be conveyed back along the linear trap

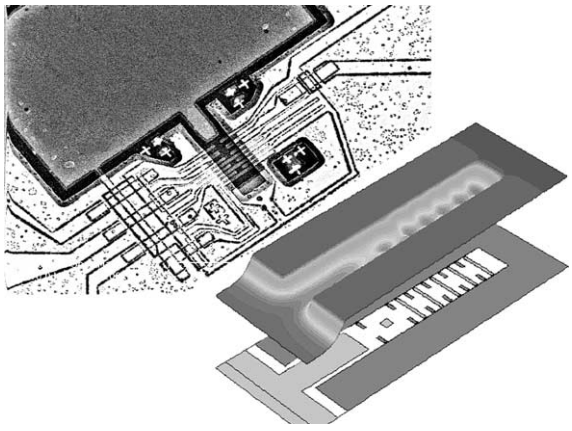

Fig. 6. (a) Schematic device for implementing QIP with electrons on helium held in a linear array of single electron traps. The calculated potential profile shows five qubits and one SET site, with a channel to the reservoir. (b) Photograph of the device presently being fabricated.

array and detected with the SET in classical time, hence reading the output register. Such a scheme could also be incorporated in a recent proposal for spin-based QIP with electrons on helium [3].

Acknowledgements

We thank A.J. Dahm, M.I. Dykman, J. Goodkind, S.A. Lyon, P.J. Meeson, P.M. Platzman and J. Saunders for discussions and F. Greenough, A.K. Betts and others for technical support. The work was supported by the EPSRC, by the EU Human Potential Programme under contract HPRN-CT-2000-00157 *Surface Electrons*, and by Royal Holloway, University of London.

References

[1] P.M. Platzman, M.I. Dykman, Science 284 (1999) 1967; M.I. Dykman, P.M. Platzman, P. Seddighrad, Phys. Rev. B 67 (2003) 155402.
[2] E. Collin, et al., Phys. Rev. Lett. 89 (2002) 245301.
[3] S.A. Lyon, cond-mat/0301581, 2003.
[4] Y. Monarkha, K. Kono, Two-Dimensional Coulomb Liquids and Solids Springer Series in Solid-State Sciences, vol. 142, Springer, Berlin, 2004.
[5] L.F. Santos, M.I. Dykman, quant-ph/0303130, 2003.
[6] M.I. Dykman, F.M. Izrailev, L.F. Santos, M. Shapiro, cond-mat/0401201, 2004.
[7] S.C. Benjamin, S. Bose, Phys. Rev. Lett. 90 (2003) 247901.
[8] S.C. Benjamin, New J. Phys. 6 (2004) 61.
[9] A.G. Fowler, S.J. Devitt, L.C.L. Hollenberg, quant-ph/0402196, 2004.
[10] P. Glasson, et al., Phys. Rev. Lett. 87 (2001) 176802.
[11] N.M. Zimmerman, W.H. Huber, A. Fujiwara, Y. Takahashi, Appl. Phys. Lett. 79 (2001) 3188.
[12] V.M. Bedanov, F.M. Peeters, Phys. Rev. B 49 (1994) 2667.
[13] M.E. Raikh, L.I. Glazman, L.E. Zhukov, Phys. Rev. Lett. 77 (1996) 1354; A.A. Koulakov, B.I. Shklovskii, Philos. Mag. B 77 (1998) 1235.
[14] R.C. Ashoori, et al., Phys. Rev. Lett. 68 (1992) 3088.
[15] G. Papageorgiou et al. cond-mat/0405084, 2004.
[16] A.A. Koulakov, F.G. Pikus, I. Shklovskii, Phys. Rev. B 55 (1997) 9223.
[17] H. Dehmelt, Science, 247539; M.F. Bartusiak, et al., A positron named Priscilla, National Academic Press, Washington, 1994.
[18] D.J. Wineland, et al., Philos. Trans. R. Soc. Lond. A 361 (2003) 1349–1361.